"Semi-submersible" 石油試錐船(浮體海洋構造物)의 運動

———計算方法, 解析 및 應用———

鄭 鎭 秀*

Motions of Semi-submersible Drilling Rigs in Deep Water

by Jin S. CHUNG*

要 約

Semisubmersible 해양석유시추선의 기본설계에 필요한 波浪中에서의 運動을 計算하는 理論的方法을 제시하고 "MOHOLE"과 "SEDCO 135-F" 석유시추선들의 運動을 해석했다. 이 규칙파에서의 운동계산을 불규칙해양波에 적용하는 응용해석을 보여주었다. 현재 이론적 방법으로는 6自由度의 운동을 해양파의 어떤 방향에 대해서도 정확히 계산할 수 있으며 계산의 정확성은 水槽에서의 모형선의 운동측정치와 實船의 운동측정치와 비교하여 증명되었다. 또 현재의 방법은 종전에 개발된 방법보다 더 一般的인 경우를 다룰 수 있으며 결과치도 더 정확하다.

극소운동특성을 갖는 해양석유시추선과 浮體해양구조물의 설계는 경비가 비싸고 시간이 많이 드는 모형실험보다는 流體力學的 Parameters를 신속 정확히 자주 변경 검토해야하는 기본설계단계에서는 정확한 이론적인 전자계산기에 의한 계산방법이 절실히 필요하다. 豫想과 같이 附加質量과 減衰力은 Resonance 운동주기에서만 운동에 영향을 준다. 해양구조물에 작용하는 波力은 Froude-Krilov force, 附加質量 및 減衰力과 Restoring force로 구성했으며 規則波에서의 6自由度 운동방정식은 본 논문에 제시된 실험측정値와 실험으로 정확도가 증명된 이론値의 부가질량과 감쇠력 係數를 써서 풀었다. 規則波에서의 계산된 운동을 Pierson-Moskowitz 海洋波 스펙트럼과 linear superposition principle에 의해 不規則海洋波에서의 운동을 계산하는데 사용했다. 不規則波에서의 운동은 운동스펙트럼과 통계적 운동치로 나타냈다.

현재의 계산방법은 실제 기본설계에 사용되어 왔으며, 다른 응용분야는 波浪中에서의 波面과 Deck 間의 Clearance, 係留線의 動張力계산의 기본 Data 및 기본설계의 Draft 등 Parameters를 通한 Optimum Design 等이다. 波의 한 方向에 對한 電子計算機(IBM 370 또는 CDC 6400)에 의한 운동계산은 10秒미만밖에 안걸린다. 또 현재의 계산방법은 해양석유시추선뿐 아니라 이와 비슷한 浮體해양구조물과 Pipe-laying 船 또 Supply Boat 設計에도 쓰여지고 있다.

NOTATION

A=incident wave amplitude (half the regular wave height)

a=radius of cylindrical member or characteristic cross-sectional dimension

A_{ij}=added mass coefficients in the equations of motion

b=vertical distance of the rig C.G. above calm water-line

B_{ij}=damping coefficients in the equations of motion

C_{xi}, C_{yi}, C_{zi}=linear viscous and wave damping forces on the i^{th} column in the x-, y-, and z-directions, respectively

c=subscript to denote pertinence to column members

C_{ij}=restoring force coefficients in the equations of motion

C_d=viscous drag coefficient

D=viscous drag or damping force

d_{ci}=diameter of the i^{th} column

d_{hi}=diameter of the i^{th} hull

E_l=wave energy

E_r=motion energy

Received : October 3, 1974

*Member; Visiting Professor, Dept. of Naval Architecture, College of Engineering, Seoul National University, Seoul, Korea.

g=gravity acceleration
H_i=wetted length of the i^{th} column
H_{xi}, H_{yi}, H_{zi}=linear viscous and wave damping forces for the i^{th} hull in the x-, y-, and z- directions, respectively
$H_{1/3}$=significant wave height (average of the 1/3-highest wave heights)
h=hulls as a subscript
h=water depth
I_x, I_y, I_z=rig moment of inertia about the x-, y-, and z-axes, respectively
k=wave number
L_i=length of the i^{th} hull
M=rig mass
m_{ci}=mass displaced by the i^{th} column
m_{hi}=mass displaced by the i^{th} hull
$\Delta m_{xci}'$, $\Delta m_{yci}'$ and $\Delta m_{zci}'$=added mass of the i^{th} column in the x-, y-, and z-directions, respectively
$\Delta m_{xhi}'$ $\Delta m_{yhi}'$ and $\Delta m_{zhi}'$=added mass of the ith hull in the x-, y-, and z-directions, respectively
$R_r(\omega)$=transfer function
$R_s(\omega)$=response motion energy spectrum density
$S_1(\omega)$=wave spectral energy density
T=wave period (sec)
t=time
V=velocity of a rig motion
X, Y, Z=force components on the rig in the x-, y-, and z-directions, respectively
(x, y, z)=cartesian coordinate system fixed in space
(x_{ci}, y_{ci})=location of the i^{th} column in the (x_i, y_i, z_i) coordinates
z_{hi}=the vertical distance of the hull axis below the rig C. G.
α=angle of incoming wave direction relative to the (x, y, z) coordinates
β_i=angle of incoming wave direction relative to the (x_i, y_i, z_i)
γ_i=angle between the x- and x_i-axis
ε_j=phase angles for the j^{th} mode of motions
ξ, η, ζ=rectilinear translational amplitudes which correspond to surge, sway, and heave, respectively
ϕ, θ, Ψ=angular rotations which correspond to roll, pitch, and yaw, respectively
ρ=sea water density
ζ=wave profile
$\tau_i=k_1x_c - k_2y_{ci} - \omega t$
χ=mean double amplitude of the rig member oscillating displacement
ω=wave frequency in rad/sec
ω=dimensionless frequency ($\omega=\omega^2a/g$)
μ_{ij}=segmental or two dimensional added mass coefficient on the i^{th} segment for the j^{th} mode of motions
λ_{ij}=segmental or two dimensional wave damping coefficient on the i^{th} segment for the j^{th} mode of motions

INTRODUCTION

There are basically four types of offshore drilling rigs (Fig. 1); fixed platform, jack-up, surface vessel, and column-stabilized semisubmersible rig. As the drilling water depth gets deeper, the fixed platforms and jack-up rigs are being replaced by the surface vessels and semisubmersible rigs. Of the surface vessels and semisubmersible rigs, recent trend of rig contructions indicates that more column-stabilized or semisubmersible rigs have been built than the surface vessels,due to the fact that motions of the semisubmersible rigs are much smaller than the surface vessel motions (Fig. 2).

In design of many floating ocean structures such as semisubmersible drilling rigs, to have small rigs' motion amplitudes is required to conduct safe, econo mical, floating (drilling) operations. The heave and-other modes (roll, pitch, surge, sway, and yaw) of large amplitudes are undesirable by restricting the handling of drill pipes, risers, etc, resulting in an increase of costly drilling downtime. According to the current floating drilling operational experiences, the maximum allowable heave in double amplitude is limited to about 10 feet and the maximum allowable roll and pitch in double amplitude are limited to about 4 degrees. To design a floating rig with minimum motion characteristics and reduce the need for expensive, time-consuming model tests, a method of accurately predicting motions of a rig at sea is a good engineering tool in the preliminary design and is presented in this paper for a case of deep water.

One of the earliest works on the motions of semisubmersible rigs is Bain's [1] which was developed for Project MOHOLE and is similar in approach to the present method, but treated only the case of parallel hulls of the column-stabilized rig. Later, Burke [3] used a direct extension method to a floating

structure of Morison's empirical wave force equaton [14], which was determined with a coordinate system fixed in a structure fixed to the water bottom. Later, Reference [13] presented a method similar to the reference [3], and both calculations by the References [3, 13] did not show all six degrees-of-freedom motions. Also the Reference [13] treated only a particular rig. References [8, 10] used strip methods which are only slightly different between the two methods. Reviewing the results obtained by these previous works, the last three methods show little improvements in the accuracy of motion calculations over the first two methods. Therefore the first two calculations [1, 3] were compared with the present calculations. Note that the method used for the Reference [12] is that of the Reference [1].

Also these previous works except the Reference [8], for the motion calculation, used constant-value added mass coefficients which are valid only for infinite fluid and consequently neglected wave damping coefficients. The References [1, 3, 13] semiempirically included viscous drag force for which the damping force term required a guessing of rig's motion velocity. The Reference [8] used frequency-dependent added mass and wave damping coefficients [11], but neglected viscous damping effects and did not show calculations for a rig with arbitrary arrangements of hull and column members relative to the wave directions. The Reference [10] presented total added mass for an entire rig, but never used it, or could not use it for his motion calculations.

The present paper derives exact linear equations of wave forces and motion with the coordinate system fixed in space for a floating structure undergoing six degrees-of-freedom motion at sea. The present method is similar in principle to and more general than the Reference [1], can handle almost all types of existing semisubmersible and multihull structures, treats arbitrary arrangements of hull and column members, and also shows a way to cut computer time required for the calculations. Also the the present motion calculations use real, accurate added mass coefficients, include wave damping coefficients and semi-empirical viscous damping coefficients, which are linearized and do not require guessing.

EQUATIONS OF MOTION AND WAVE FORCE

Consideration of the Problem

Most semisubmersible (floating) rigs consist mainly of tubular, cylindrical structural members with various cross-sectional shapes. These members are either submerged or semisubgerged. Wave forces acting on these members induce rig motions. The arrangement of these submerged members differs from one design to another, causing different rig motions for given sea states.

The amplitudes and slopes of the incident waves are assumed to be so small that the waves may be described as infinitesmal waves. A rig is asumed to undergo a small-amplitude, rigid-body motion with six degrees of freedom in waves. Sufficient distance is assumed between adjacent supporting members so that the hydrodynamic interference effects between adjacent columns or hulls can be neglected. Also the members are idealized as a group of many tubular T-segments consisting of a column and a hull (Fig. 3); the member parallel to the mean free surface is called a hull, and that normal to the mean free surface a column. The hydrodynamic treatment of the rig is made on each tubular T-segment, neglecting the hydrodynamic interference by the T-joints.

The present wave forces consist of Froude-Krilov forces (forces exerted by incoming waves and assumed to be undisturbed by the presence of the members), added mass forces, wave and linearized viscous damping forces, and hydrostatic forces. Reflected wave systems caused by the presence of the rig members are small and are neglected.

A cartesian coordinate system (x, y, z) is fixed in space with its origin at the center of gravty (CG) of a rig (Fig. 3). The x-axis is positive forward, the y-axis is positive toward port, and the z-axis positive upward. Another coordinate system (x_i, y_i, z_i) is introduced with its origin at $z=0$ of the i^{th} T-segment. The x_i-axis is along the hull axis, and there is an angle γ_i in the horizontal plane between the x-and x_i-axes for a hull which can have any angle relative to the wave heading. When submerged members including the hulls are parallel to each other or $x \parallel x_i$, $\gamma_i=0$. The $\gamma_i \neq 0$ allows any orientation of the submerged members relative to the wave heading. The

vertical axis of the i^{th} T-segment is perpendicular to the plane of $x=x_{ci}$ and $y=y_{ci}$, where the subscript "c" stands for a column and the subscript "h" will be used for hull.

Let ξ, γ, and ζ be the rectilinear translational displacements corresponding to surge, sway, and heave, respectively, and ϕ, θ, and Ψ the angular rotations about the rig CG corresponding to roll, pitch, and yaw. Thus the translational displacements for a point located at z_i are expressed in the form of

$$\xi_i=(\xi+z_i\theta-y_{ci}\Psi)\cos\gamma_i+(\gamma+x_{ci}\Psi-z_i\phi)\sin\gamma_i, \quad (1)$$

$$\gamma_i=(\gamma+x_{ci}\Psi-z_i\phi)\cos\gamma_i-(\xi+z_i\theta-y_{ci}\Psi)\sin\gamma_i, \quad (2)$$

and

$$\zeta_i=\zeta+y_{ci}\phi-x_{ci}\theta \quad (3)$$

Note that Eqs. (1) and (2) will have only the first bracket terms when hulls and bracing members are parallel to the x-axis (or $\gamma_i=0$).

Let the incoming wave elevation be in the following form,

$$\xi(x,y,z(x,y);t)=Ae^{k(z+b)}\cos(k_1x-k_2y-\omega t) \quad (4)$$

for infinitely deep water, and wave number is defined as

$$k=\frac{\omega^2}{g} \quad (5)$$

where A=wave amplitude (half the regular wave height); b=vertical distance from the mean water surface to the rig VCG; $k_1=k\cos\beta_i$; $k_2=k\sin\beta_i$; ω=the circular wave frequency in rad/sec and is the same as the frequency of the rig response in waves; and g=gravity acceleration.

Assuming that the port and starboard of a rig are

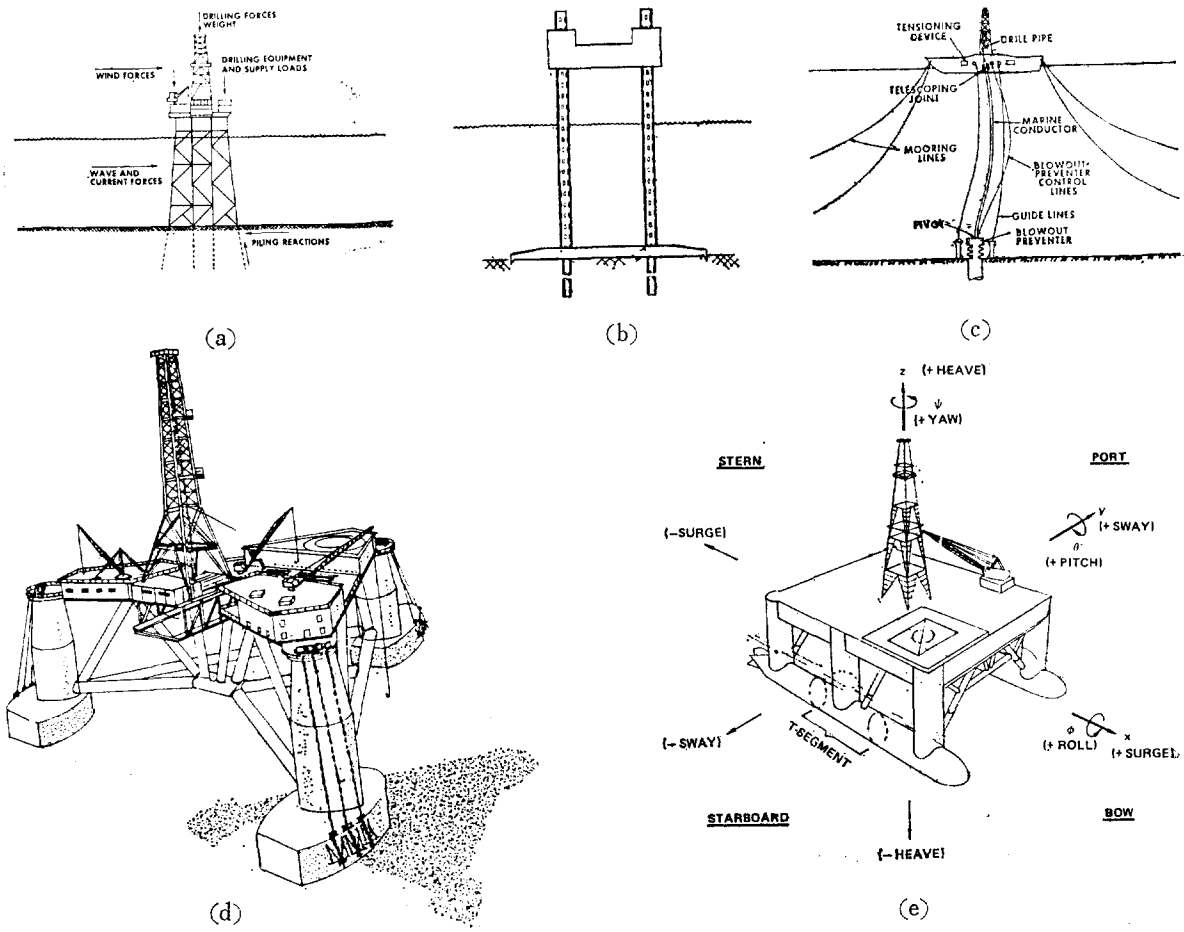

Fig. 1 Four Basic Types of Offshore Drilling Rigs
(a) Fixed Platform
(b) Jack-up Rig
(c) Ship
(d) Semisubmersible-"SEDCO 135-F"
(e) Semisubmersible-"MOHOLE"

symmetric about the longitudinal axis of the rig CG, the equations of motion are expressed in a general form of

$$\sum_{k=1}^{6}\left[(M_{jk}+A_{jk})\frac{d^2xk}{dt^2}+B_{jk}\frac{dx_k}{dt}+C_{jk}x_k\right]=F_j \qquad (6)$$

where

$$x_k=\begin{pmatrix}\xi\\ \eta\\ \zeta\\ \phi\\ \theta\\ \psi\end{pmatrix}\begin{matrix}\text{surge}\\ \text{sway}\\ \text{heave}\\ \text{roll}\\ \text{pitch}\\ \text{yaw}\end{matrix} \qquad (7)$$

and M_{jk} are the components of the generalized mass matrix for the rig, A_{jk} and B_{jk} are the added mass and damping coefficients, C_{jk} are the hydrostatic restoring coefficients, and F_j are the exciting forces and moments. F_1, F_2, and F_3 refer to the surge, sway, and heave exciting forces, while F_4, F_5, and F_6 are the roll, pitch, and yaw exciting moments.

The generalized mass matrix of the rig is given by

$$M_{jk}=\begin{pmatrix} M & 0 & 0 & 0 & 0 & 0\\ 0 & M & 0 & 0 & 0 & 0\\ 0 & 0 & M & 0 & 0 & 0\\ 0 & 0 & 0 & I_4 & 0 & 0\\ 0 & 0 & 0 & 0 & I_5 & 0\\ 0 & 0 & 0 & 0 & 0 & I_6 \end{pmatrix} \qquad (8)$$

where M is the mass of the rig, I_j is the moment of inertia in the j^{th} mode ($j=4,5,6$). Other components in Eq.(8) vanish, since the origin of the coordinate system (Figs. 1 and 3) is the same as the rig's CG and the rest of the compenents are zeros or very small (neglected).

The added mass (or damping) coefficients for the rig are

$$A_{jk}(\text{or } B_{jk})=\begin{pmatrix} a_{11} & a_{12} & 0 & a_{14} & a_{15} & a_{16}\\ a_{21} & a_{22} & 0 & a_{24} & a_{25} & a_{26}\\ 0 & 0 & a_{33} & a_{34} & a_{35} & 0\\ a_{41} & a_{42} & a_{43} & a_{44} & a_{45} & a_{45}\\ a_{51} & a_{52} & a_{53} & a_{54} & a_{55} & a_{56}\\ a_{61} & a_{62} & 0 & a_{64} & a_{65} & a_{66} \end{pmatrix} \qquad (9)$$

Furthermore, the hydrostatic restoring force coefficients for the rig are

$$C_{jk}=\begin{pmatrix} 0 & 0 & 0 & 0 & 0 & 0\\ 0 & 0 & 0 & 0 & 0 & 0\\ 0 & 0 & C_{33} & C_{34} & C_{35} & 0\\ 0 & 0 & C_{43} & C_{44} & 0 & 0\\ 0 & 0 & C_{53} & 0 & C_{55} & 0\\ 0 & 0 & 0 & 0 & 0 & 0 \end{pmatrix} \qquad (10)$$

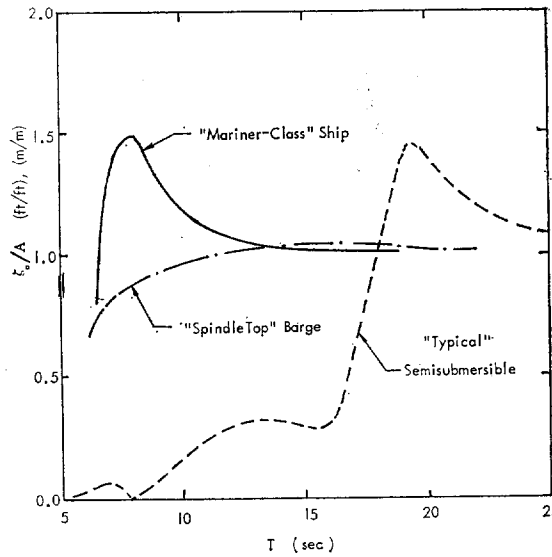

Fig. 2 Heave-Motion Comparison for Barge, Ship, and Semisubmersible Drilling Vessels

For the stationary rig, the coefficients are symmetric; $A_{jk}=A_{jk}$, $B_{jk}=B_{kj}$, and $C_{jk}=C_{kj}$. In order to

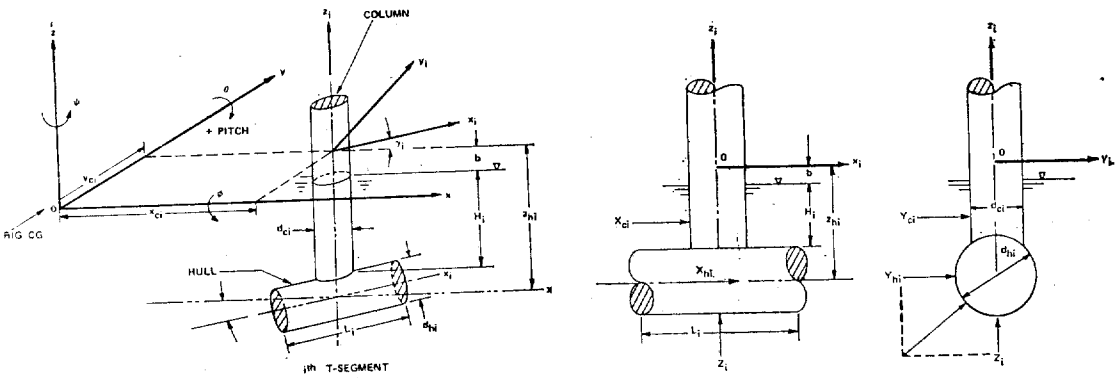

Fig. 3 The Coordinate Systems and Definition of Force Components

determine the coefficientt in Eqs. (9) and (10), the equations of total wave force on the individual T-segments in the three orthogonal directions are first derived and then equated to the rig mass acceleration product, which follows in the next sections. This leads to simultaneous ordinary linear differential equations of motion, and the solution gives x_k, $k=1, 2, \cdots\cdots 6$: surge, sway, heave, roll, pitch, and yaw motions in regular waves (see Eq. (7)).

Froude-Krilov Forces and Hydrostatic Forces

The pressure is given by Bernoulli equation, neglecting the higher order terms,

$$p=\rho gz-\rho\frac{\partial\Phi}{\partial t}+\text{constant} \tag{11}$$

where g=gravity acceleration; ρ=water density; Φ=velocity potential.

The kinetic and dynamic condition on the free surface are expressed in a combined form of

$$\frac{d\phi}{dt}=\frac{g}{\omega^2}\frac{d^2\zeta}{dt^2}=0 \tag{12}$$

The substitution of Eq. (12) into Eq. (11) gives

$$-p=g(-x+z+y)+A\rho e^{k(z+b)}\cos(k_1x-k_2y-\omega t) \tag{13}$$

for infinitely deep water.

For later use, derivatives of Eq. (13) are taken to be in the form of

$$-\frac{\partial p_i}{\partial x}=-\rho g\theta-\rho A\omega^2e^{k(z+b)}\cos\beta_1\ \sin\tau_i \tag{14}$$

$$-\frac{\partial p}{\partial y}=\rho g\phi+\rho A\omega^2e^{k(z+b)}\sin\beta_i\ \sin\tau_i \tag{15}$$

$$-\frac{\partial p_i}{\partial z}=\partial g+\rho A\omega^2e^{k(z+b)}\sin\tau_i \tag{16}$$

where $\beta_i=\alpha+\gamma_i$; α=angle of incident wave direction relative to the hull (x_i-) axis in the x-y plane, $\alpha=\pi/2$ for beam waves, $\alpha=\pi$ for head waves; and $\tau_i=k_1x-k_2y-\omega t$.

Integration of the pressure over the cross-sectional area, or using Green's theorem with the pressure dervatives, Eqs. (14) to (16), one obtains the Froude-Krilov forces and the hydrostatic forces

$$x_i=\iint_{Si}P_i\cos(n,x)dS_i=-\iiint_{Vi}\frac{\partial p_i}{\partial x}dV_i \tag{17}$$

$$y_i=\iint_{Si}p_i\cos(n,y)dS_i=-\iiint_{Vi}\frac{\partial p_i}{\partial y}dV_i \tag{18}$$

and

$$z_i=\iint_{Si}p_i\cos(n,z)dS_i=-\iiint_{Vi}\frac{\partial p_i}{\partial z}dV_i \tag{19}$$

where S_i and V_i are the cross-sectional area and volume of the i^{th} T-segment, respectively.

Since members of most semisubmersible rigs have cross-sectional dimensions which are very small compared to the wave length, the T-segment can be represented as displaced mass of a column and a hull. This approximation greatly simplifies the pressure integrals without losing accuracy and greatly reduces the computer time. Thus, the Froude-Krilov forces and hydrostatic forces on the i^{th} T-segment (Fig. 3) obtained from Eqs. (17) to (19) are

$$x_{ci}=m_{ci}\omega^2AQ_0(k)\cos\beta_i\sin\tau_i \tag{20}$$

$$y_{ci}=-m_{ci}\omega^2AQ_0(k)\sin\beta_i\ \sin\tau_i \tag{21}$$

$$z_{ci}=-(m_{ci}\omega^2Q_0(k)-\rho gS_{ci})A\cos\tau_i-\rho gS_{ci}z_{ci} \tag{22}$$

$$x_{hi}=m_{hi}\omega^2AI_i(k)\cos\beta_i\ \sin\tau_i \tag{23}$$

$$y_{hi}=-m_{hi}\omega^2AI_i(k)\sin\beta_i\ \sin\tau_i \tag{24}$$

$$z_{hi}=-m_{hi}\omega^2AI_i(k)\cos\tau_i-gS_{hi}z_i \tag{25}$$

where m_{ci}=displaced mass of the i^{th} column; m_{hi}=displaced mass of the i^{th} hull;

$$Q_0(k)=(1-e^{-kh}i)kH_i \tag{26}$$

for infinitely deep water; L_i, H_i=submerged lengths of the i^{th} hull and column, respectively; S_{ci}, S_{hi}=cross-sectional areas of the i^{th} column and hull. respectively;

$$I_i(k)=\sin(\frac{kL_i}{2}\cos\beta_ie^{-k}(z_{hi}-b)/(kL_i/2)\cos\beta_i \tag{27}$$

for infinitely deep water;

$$z_1\text{ or }z_c=\frac{1}{H_i}\int_{Hi}zdz;$$

and z_{hi}=the mean vertical distance from the rig CG to the center of buoyancy of the i^{th} hull. With the assumption of small θ and Ψ in Eqs. (14) to (16), the hydrostatic forces associated with θ and Ψ are small and are neglected in Eqs. (20) to (25) which are wave forces under the Froude-Krilov hypothesis and the hydrostatic force.

A rig's oscillating motion in response to the incoming waves generates additional pressure gradients by a change of the acceleration and velocity field in the fluid, which corresponds to the forces due to the added mass and wave damping coefficients. These forces together with the Froude-Krilov forces and hydrostatics forces are the total wave forces acting on the member and are discussed in the next sections.

Added Mass and Damping Forces

Added Mass and Damping Coefficients: the forced wave system generated by the rig motions changes the pressure field around the submerged portion of members, due to the body motion-wave interaction

and the bottom-depth effect, in addition to the pressure field generated by tue member motion in infinite fluid. The pressure component in phase with the acceleration is the added mass component, and the component in phase with the velocity is the wave damping component. The resulting forces are added mass and damping forces on the members. The wave damping coefficient λ_{ij} is connected with the energy dissipation due to surface waves generated by the member during rig's oscillating motions.

When a submerged member oscillates close to the water-bottom boundary, the added mass and damping coefficients are influenced by both the water depth and free surface effects. The frequency range of interest for the submerged members of the ordinary floating drilling structure for the operational and survival sea states is from $\omega=\omega^2\ a/g=0.05$ to 2.0 where ω is the rig's motion frequency in rad/sec and is the same as the wave frequency and a is a diameter of characteristic cross-sectional dimension of the rig members.

Fig. 4 shows experimentally determined added mass and wave damping coefficients for a model of submerged oval with vertical circular cylinder; the oscillation experiment was carried out with planar motion mechanism, and the oscillation amplitudes were kept linear against the total force measured.

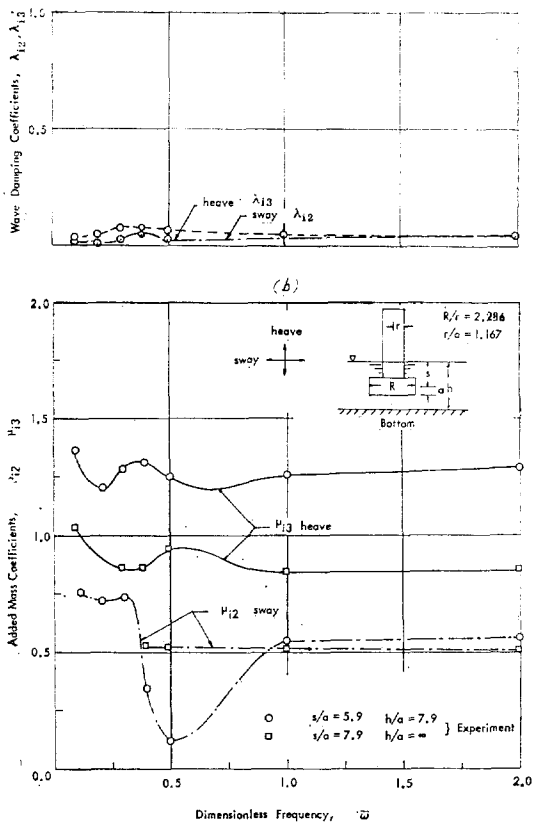

Fig. 4(a) Heave and Sway Added Mass Coefficients for a Model of Submerged Oval with Vertical Circular Cylinder

Fig. 4(b) Heave and Sway Wave Damping Coefficients for a Model of Submerged Oval with Vertical Circular Cylinder

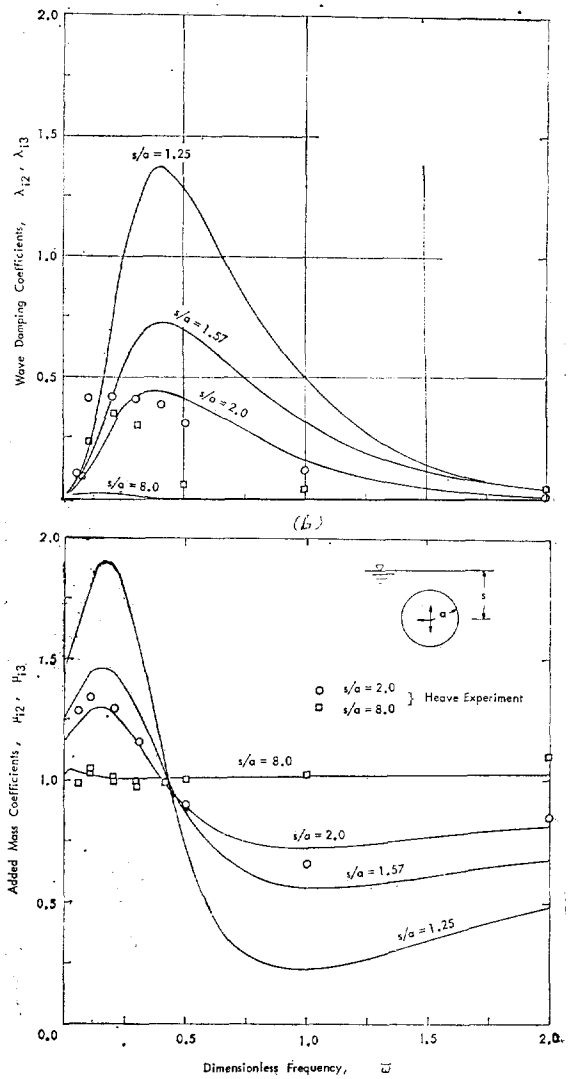

Fig. 5(a) Heave and Sway Added Mass Coefficients for a Model of Submerged Horizontal Circular Cylinder (Deep Water)

Fig. 5(b) Heave and Sway Wave Damping Coefficients for a Model of Submerged Horizontal Circular Cylinder (Deep Water)

Although submergence ratios s/a of Fig. 4 are different between the finite-water depth test and the infinite-depth test, the test data clearly indicate, (a) that the heave added mass coefficients for the finite depth are larger than the heave coefficients for the infinite depth, (b) that for the heave coefficients the free surface effect becomes negligibly small when s/a≥6.0 and for the sway coefficients the free surface effect becomes little when s/a≥8.0, and (c) that the sway coefficients are only slightly larger at higher frequency range than the sway coefficient for the infinite depth. The free surfaces and water depth effects significantly influence the sway coefficients over the frequency range of interest. The closer to the bottom the model oscillates, the larger both the heave and sway coefficients become. As ω increases, the added mass coefficients for the finite depth generally become larger than the coefficients for the infinite depth.

Fig. 5 shows both theoretically [11] calculated and limited, experimentally determined, heave added mass and wave damping coefficients for a submerged model of horizontal circular cylinder in infinitely deep water. Comparison of the calculations with limited expermental points for s/a=2.0 [4] shows good agreement except for damping. The theoretical basis of Reference [11] permits to assume that the calculated coefficients are accurate for at least s/a≥2.0. Also unpublished experimental data for s/a≥6.0 for finite-depth water [4] show that the free surface effect on or frequency dependence of the coefficients becomes practically zero for both heave and sway oscillations. Thus the above information leads to a conclusion that the free surface effect on both the heave and sway coefficients for s/a≥5.0 becomes very small and can be neglected for the motion calculations: the wave damping coefficients become zero and the added mass coefficients become a constant.

In design and operational practice s/a=3~4 for the drilling draft of many semisubmersible rigs such as the MOHOLE rig with circular cylindrical hulls and s/a=1.5~2.0 for the survival draft. For the MOHOLE rig, the drilling draft ranges 60ft (18.29m) to 70 ft (21.34m) corresponding to s/a=2.43~3.0, and the survival draft is 45 ft (13.72m) corresponding to s/a=1.57. Thus the present motion calculations use the added mass and wave damping coefficients calculated on the basis of Reference [11].

The added masses on the column and hull of the i^{th} segment in the x_j-, y_i-, and z-directions are defined in terms of the segment mass and added mass coefficients,

$$\Delta m_{xci},\ \Delta m_{yci},\ \Delta m_{zci}=m_{ci}(\mu_{ci})_{x,y,z} \tag{28}$$

$$\Delta m_{xhi},\ \Delta m_{yhi},\ \Delta m_{zhi}=m_{hi}(\mu_{hi})_{x,y,z} \tag{29}$$

where the added mass coefficient is defined as,

$$(\mu_{hi})_j=(\text{in-phase force})_{ij}/m_{hi}\omega^2 A \text{ for a hull and} \tag{30}$$

$$(\mu_{hi})_j=(\text{in-phase force})_{ij}/m_{ci}\omega^2 A \text{ for a column,}$$

$$j=1,2,3 \tag{31}$$

These hydrodynamic coefficients affect the rig motions only near resonance as will be discussed later. The added mass and wave damping coefficients μ_{ij} and λ_{ij}, respectively are a function of the rig-oscillation frequency and direction, geometry of the hull and column members, submerged distance of the member from the free surface, and the water depth according to Reference [4].

Besides the added mass and wave damping forces, viscous damping influences the rig motions through the Reynolds number effect. The viscous damping effect on the motions is significant only near resonance periods. For an oscillating rig, velocity can be determined from the frequency and amplitude of the rig's oscillations. As a basis for using the wind tunnel data for drag coefficients C_d, a Reynolds number is introduced as

$$R=\frac{lV}{\nu} \tag{32}$$

where $V=\omega\chi\cos(\omega t-\epsilon)$; ω=circular frequency of the rig oscillation: χ=mean double amplitude of rig member oscillation: ν=dynamic viscosity: l=principal dimension of the rig member normal to the direction of the motion: and ϵ=phase angle.

The linearized viscous drag [2] on the i^{th} column and hull is

$$D_{ci,hi}=\frac{4}{3\pi}C_d p S_{ci,hi} V \tag{33}$$

where $S_{ci,hi}$=the principal projected area of the i^{th} column and hull segment, respectively.

C_d is drag coefficient obtained in general format by normalizing the drag without the factor $8/3\pi=0,8488$,

The linearized total damping force component for the i^{th} column and hull segment is expressed in the

form of

$$C_{xi},\ C_{yi},\ C_{zi}=\frac{4}{3\pi}C_d S_{ci}\omega(\chi_{ci})_{x,y,z})+(\lambda_{ci,x,y,z}m_{ci}\omega \tag{34}$$

$$H_{xi},\ H_{yi},\ H_{zi}=\frac{4}{3\pi}C_d S_{hi}\omega(\chi_{hi})_{x,y,z})+(\lambda_{hi,x,y,z}m_{hi}\omega \tag{35}$$

where

$(X_{ci})_{x,y,z}$, $(\chi_{hi})_{x,y,z}$ = the mean double amplitudes of the motions of the i^{th} column and hull segment in x-, y-, and z- directions, respectively; and

$(\lambda_{ci})_{x,y,z}$, $(\lambda_{hi})_{x,y,z}$ = the wave damping coefficients of the i^{th} column and hull in the x-, y-, and z-directions, respectively;

i is the i^{th} member segment number. The first terms in Eqs. (34) and (35) are the linearized viscous damping force component as defined in Eq. (33). In nonlinear equations of motion, the viscous drag or damping coefficient C_d is associated with the quadratic velocity term. But in the present linear equations of motions, C_d is associated with a linear velocity term.

Mathematical Derivation of Added Mass and Damping Forces: since the diameters of the hull and column members of the rig are small compared to the incoming wavelength, the motion of the water surface is assumed to be uniform across the member diameters. The velocity components of the water particle in the y-direction relative to the i^{th} column at z_i is

$$V_{yci}=-A\omega e^{k(z_i+b)}\cos\tau_i\ \sin\beta_i-\gamma_{ci} \tag{36}$$

where the motion of the column is defined as

$$\xi_{ci}=(\xi+\xi_{ci}\theta-Y_{ci}\Psi)\cos\gamma_i+(n+x_{ci}\Psi-z_{ci}\phi)\sin\gamma_i \tag{37}$$

$$n_{ci}=(n+x_{ci}\Psi-z_{ci}\phi)\cos\gamma_i-(\xi+\xi_{ci}\theta_{ci}\Psi)\sin\gamma_i$$

and

$$\zeta_i=\zeta+y_{ci}\phi-x_{ci}\theta$$

Other notations are defined previously. A dot over the displacement variables indicates the first derivative with respect to time t. Similarly, the velocity components V_{xci} and V_{zci} in the y-and z-directions, respectively are obtained. Similarly, the accelerations of water particles relative to the i^{th} column can be obtained upon taking the derivative of the velocity components of Eq. (36) with respect to time.

The added mass force on the i^{th} column in the y_i-direction due to the acceleration of water particles relative to the i^{th} columnis obtained by integrating the acceleration with respect to z_i,

$$\frac{\Delta m_{yci}}{H_i}\int_{-(H_i+b)}^{-b}\dot{V}_{yci}dz_i=-\Delta m_{yci}\{A\omega^2Q_o(k)\cos\beta_i\ \sin\tau_i+\ddot{\eta}_{ci}\} \tag{38}$$

and the corresponding damping force is obtained from Eq. (36).

$$\frac{C_{yi}}{H_i}\int_{-(H_i+b)}^{-b}V_{yci}dz_i=-C_{yi}\{A\omega Q_o(k)\cos\beta_i\ \cos\tau_i+\dot{\eta}_{ci}\} \tag{39}$$

where Δm_{yci} and C_{yi} are the added mass and the damping forces, respectively.

Thus, the added mass and damping forces acting on the i^{th} sfgment in the (x_i,y_i,z_i) coordinate are expressed in the following form:

$$X_{ci}=(\Delta m_{xci}\ddot{\xi}_{ici}+C_{xi}\dot{\xi}_{ci})+\Delta m_{xci}\omega^2AQ_o(k)(\cos\beta_i\ \sin\tau_i+C_{xi}\omega AQ_o(k)\cos\beta_i\ \cos\tau_i \tag{40}$$

$$X_{hi}=-(\Delta m_{xhi}\ddot{\xi}_{hi}+H_{xih}\dot{\xi}_i)+\Delta m_{xhi}\omega^2AI_i(k)\cos\beta_i\cos\tau_i+H_{xi}\omega AI_i(k)\cos\beta_i\ \cos\tau_i \tag{41}$$

$$Y_{ci}=-(\Delta m_{yci}\ddot{\xi}_{ci}+C_{yi}\dot{\xi}_{ci})-\Delta m_{yci}\omega^2AQ_o(k)\sin\beta_i\sin\tau_i-C_{yi}\omega\ AQ_o(k)\sin\beta_i\ \cos\tau_i \tag{42}$$

$$Y_{hi}=-(\Delta m_{yhi}\ddot{\eta}_{hi}+H_y\dot{\eta}_{ihi})-\Delta m_{yhi}\omega^2AI_i(k)\sin\beta_i\sin\tau_i \tag{43}$$

$$Z_{ci}=-(\Delta m_{ci}\ddot{\eta}_i+C_{zi}\dot{\eta}_i)+C_{zi}\omega AQ_o(k)\sin\beta_i\ \cos\tau_i \tag{44}$$

and

$$Z_{hi}=-(\Delta m_{zhi}\ddot{\eta}_i+H_{zi}\dot{\eta}_i)+H_{zi}\omega AI_i(k)\cos\tau_i \tag{45}$$

A dot on top of symbols means the first derivative with respect to time, and two dots mean the second derivative with respect to time.

Total Wave Forces on T-Segments

In the previous section, the Froude-Krilov force (including the hydrostatic force) and added mass and damping forces were obtained. Upon summing these linear forces, the total wave forces acting on the i^{th} T-segment in the (x_i,y_i,z_i) coordinate can be obtained as follows.

Thus the total x_i-directional force component of the i^{th} column (χ_{ci}) is obtained as the sum of Eqs. (20) and (40). If the dimension of the column cross section is much smaller than the submerged length of the circular column, generally $m_{ci}\simeq\Delta m_{xci}\simeq\Delta m_{yci}$.

For the motion of cylindrical hull along its longitudinal axis such as that of the Project MOHOLE rig, the added mass and wave damping forces are negligible, but not for the motion of a non-cylindrical hull like the hulls of the SEDCO rig (Fig. 1). The total x_i-directional force component on the i^{th} hull (χ_{hi}) is obtained as the sum of Eqs. (21) and (41).

The total y_i-directional force component on the i^{th}

column (Y_{ci}) is the sum of Eqs. (22) and (42),

$$Y_{ci}=-(\Delta m_{yci}\ddot{\gamma}_{ci}+C_{yi}\dot{\gamma}_{ci})-(m_{ci}+\Delta m_{yci})^2AQ_e(k)\times\sin\beta_i\sin\tau_i-C_{yi}\omega AQ_e(k)\sin\beta_i\cos\tau_i \quad (46)$$

The total y_i-directional force component on the i^{th} hull (Y_{hi}) is the sum of Eqs. (23) and (43),

$$Y_{hi}=-(\Delta m_{yhi}\ddot{\gamma}_{hi}+H_{yi}\dot{\gamma}_{hi})-(m_{hi}+\Delta m_{yhi})\omega^2AI_i(k)\times\sin\beta_i\sin\tau_i-H_{yi}\omega AI_i(k)\sin\beta_i\cos\tau_i \quad (47)$$

For the hull and column of a circular cylindrical cross section, it is generally true [4] that $\Delta m_{yhi}\simeq\Delta m_{xhi}$ for the hull and $\Delta m_{xci}=\Delta m_{yci}$ for the column, and that the wave dampings have the relationship $\lambda_{yhi}\simeq\lambda_{xhi}$ for the hull and $\lambda_{xci}=\lambda_{yci}$ for the column. Project MOHOLE rig (Fig. 1) belongs to this case. For the cylinder in axial motion, the hydrodynamic inertia and damping forces are small and negligible. The total heaving forces on the i^{th} column (Z_{ci}) and hull (Z_{hi}) are obtained as the sum of Eqs. (24) and (44) and the sum of Eqs. (25) and (45), respectively.

The total wave forces derived above for the (x_i, y_i,z_i) coordinate can be rewritten for the total wave forces in the (x,y,z) coordinate

$$X=\sum_i^N X_i=\sum_{i=1}^N[(X_{ci}+X_{hi})\cos\gamma_i-(Y_{ci}+Y_{hi})\sin\gamma_i] \quad (48)$$

$$Y=\sum_i^N Y_i=\sum_{i=1}^N[(Y_{ci}+Y_{hi})\cos\gamma_i+(X_{ci}+X_{hi})\sin\gamma_i] \quad (49)$$

and

$$Z=\sum_i^N Z_i=\sum_{i=1}^N(Z_{ci}+Z_{hi}) \quad (50)$$

where N is total number of the T-segments. Note that Eqs. (48) and (49) will have only the first bracket terms when the hulls and bracing members are parallel to the x-axis (or $\gamma_i=0$). For the structural analysis, the total forces for the (x_i, y_i, z_i) coordinate can be used.

Equations of Motions

With the total wave forces derived in Eqs. (48) to (50) for the (x,y,z) coordinate the equations of motion can be expressed in the form of

$$M\ddot{\xi}=X \quad (51)$$

$$M\ddot{\eta}=Y \quad (52)$$

$$M\ddot{\zeta}=Z \quad (53)$$

$$I_x\ddot{\phi}=\sum_i^N\{-\int H_i[-\frac{d}{dz}(Y_{ci}\cos\gamma_i+X_{ci}\log\gamma_i)]z\,dz+(Y_{hi}\cos\gamma_i+X_{hi}\sin\gamma_i)Z_{hi}+Z_iY_{ci}+g(m_{hi}z_{hi}-\int H_iS_{ci}zdz)\phi\} \quad (54)$$

$$I_y\ddot{\theta}=\sum_i^N\{\int H_i[\frac{d}{dz}(x_{ci}\cos\gamma_i-Y_{ci}\sin\gamma_i)]zdz-(X_{hi}\cos\gamma_i-Y_{hi}\sin\gamma_i)z_{hi}-z_{ci}x_{ci}-\int_{Li}(\frac{d}{dx}Z_{hi})x\,dx+g(m_{hi}z_{hi}-\int H_iS_{ci}zdz)\theta\} \quad (55)$$

and

$$I_z\ddot{\Psi}=\sum_i^N\{-X_iY_{ci}+(Y_{ci}\cos\gamma_i+X_{ci}\sin\gamma_i)x_{ci}+\int_{Li}[-\frac{d}{dz}(Y_{hi}\cos\gamma_i+X_{hi}\sin\gamma_i)]x\,dx\} \quad (56)$$

where I_x, I_y, I_z=the mass moments of inertia about the x-, y-, and z-axis, respectively.

Upon substituting the total wave forces derived above into Eqs. (51) to (56) and carrying out the integration, the added mass, damping, and restoring force coefficients a_{ij}, b_{ii}, respectively and the exciting force F_j in Eq. (6) can be determined through straightforward, but tedious algebra. Upon solving Eq. (6), the six degrees-of-freedom rig motions (surge, sway, heave, roll, pitch, and yaw) in regular waves are obtained.

Motions for Regular Waves

Basic Data and Definitions. The motions calculated by the present method are compared with and validated by existing model test data [3, 12] full-scale test data [9], and previous works [1, 3].

The present motion calculations are made with Eq. (6), and the rig characteristics of the 3-column stabilized SEDCO 135-F and 6-column stabilized MOHOLE used for the present calculations are close to those [1, 3], which simulate principal dimensions and weight distribution of the prototype rigs (see Table 1). A method of calculating motions of floating drilling rigs in a finite-depth water is fortunately available [15]. Therefore, the SEDCO 135-F motions are calculated by the method of the Reference [15] for 400ft (121.92m) and 80 ft (24.38m) draft and by the present method for deep water and 75ft (22.86m) draft. The present calculations used the frequency-dependent added mass coefficients and wave damping coefficients as given in Figs. 4 and 5, viscous damping coefficient of $C_d=1.0$, and the hydrodynamic end effect of the rig member is neglected.

Reference [3] used a direct extension to a floating ocean structure of Morison's empirical wave force equation [14] determined for a fixed structure. The motion calculations by the Reference [3] use constant-value added mass coefficients which are guessed for infinite fluid, consequently neglected wave damping coefficients, and empirically included viscous damping coefficients which again require a guessing of rig's oscillating motions velocity for the damping force term in the equations of motion (Eq. (6)). Note that the Morison's equation was determined for a fixed structure so that wave damping does not exist. The Reference [1] used a method similar in approach to the present method, but treated the case of parallel hulls: his calculations for the MOHOLE rig used constant-value added mass coefficients which are valid for a circular cylinder in infinite fluid, neglected the wave damping, and viscous damping coefficient of $C_d=0.8\sim1.0$ which was not clearly explained.

A part of the model test data [3] of motion amplitudes and phase angles for the SEDCO 135-F rig were obtained for the regular waves; the water depth was 400 ft (121.92m), and the simulated rig's draft was 80 ft (24.38m). The full-scale test data [9] of motion amplitudes were obtained for the SEDCO 135-F rig off Vancouver coastline, British Columbia, Canada; the wave heading was not known, and water depths were between 180 ft (54.9m) and 330 ft (100.6m). Due to the uncertainty in the accuracy of the full-scale data for the modes of motions other than heave, only the heave (Fig. 6) is used for the present motion correlation. Also the heave amplitudes do not significantly change due to the variation of the wave headings. The model test data [12] of the MOHOLE rig were obtained for the regular waves and provided limited data of motion amplitudes only; the water depth was claimed to be infinitely deep, the simulated draft was 70 ft (21.34m), and phase angles of the motions were not analyzed.

In Figs.8 to 16 the surge (ξ), sway ( ), and heave (ζ) amplitudes in regular waves are presented as and referred to response amplitude operators, or transfer functions (R_r); ξ_a/A, η_a/A, and ζ_a/A, respectively, and the roll (ϕ), pitch (θ), and yaw (Ψ) amplitudes as transfer functions (R_r); ϕ_a/A, θ_a/A, and Ψ_a/A, respectively. These motion transfer functions are the

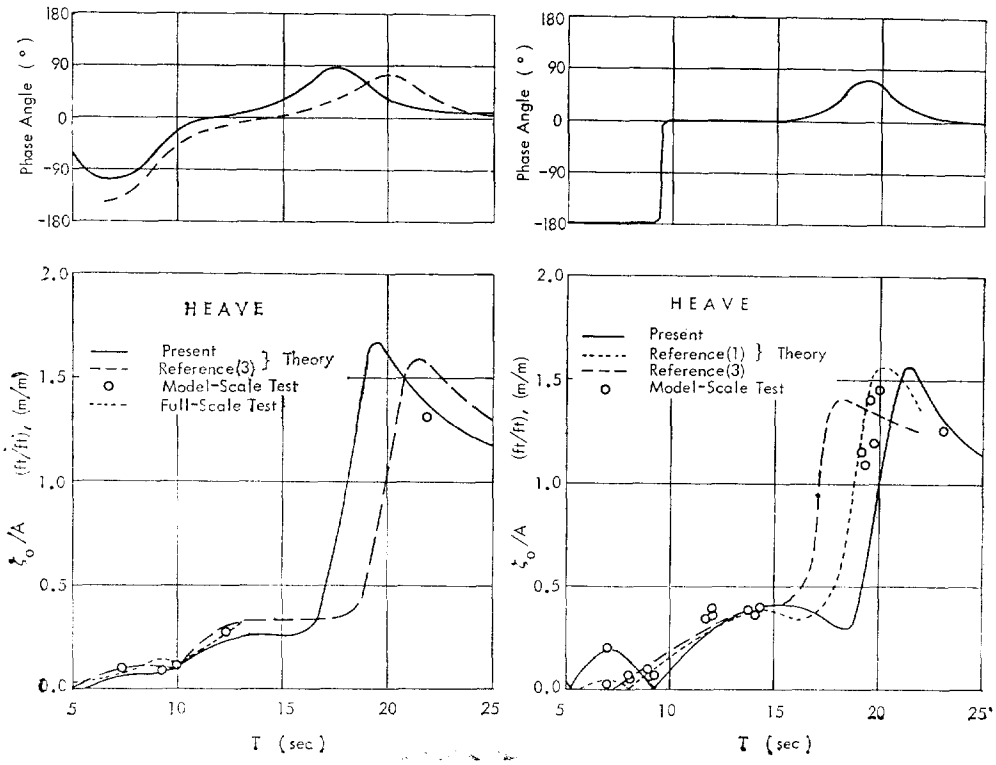

Fig. 6 Heave of SEDCO 135-F (waves 60° off bow; 400ft (121.92m) water depth)
Fig. 7 Heave of MOHOLE (beam waves; deep water)

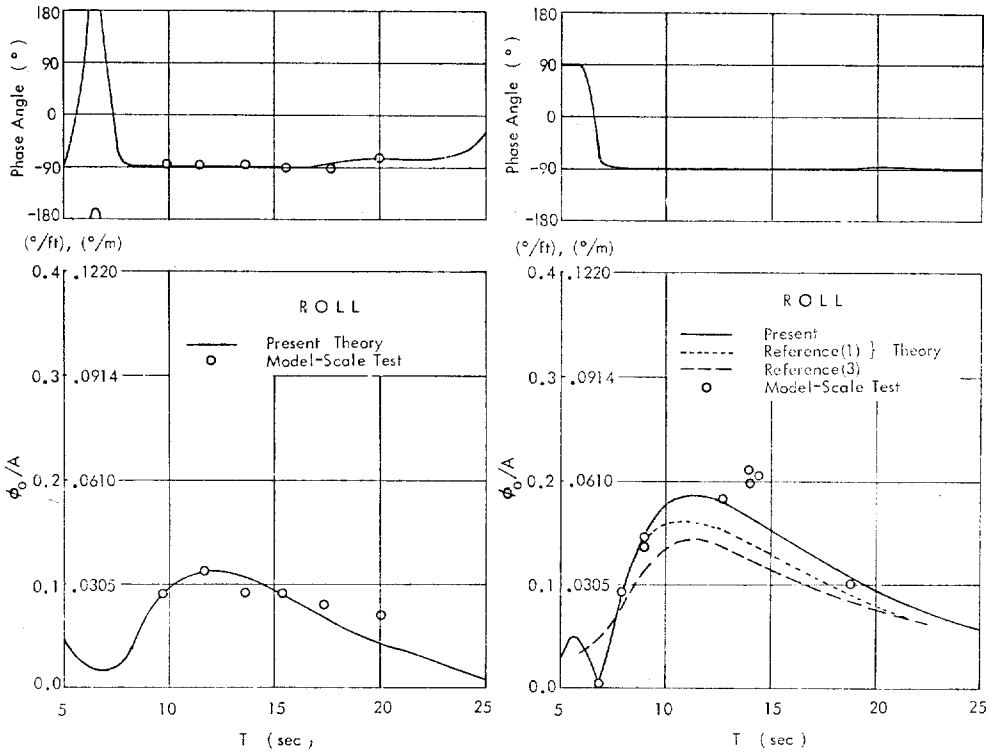

ig. 8 Roll of SEDCO 135-F (beam waves; deep water)
Fig. 9 Roll of MOHOLE (beam waves; deep water)

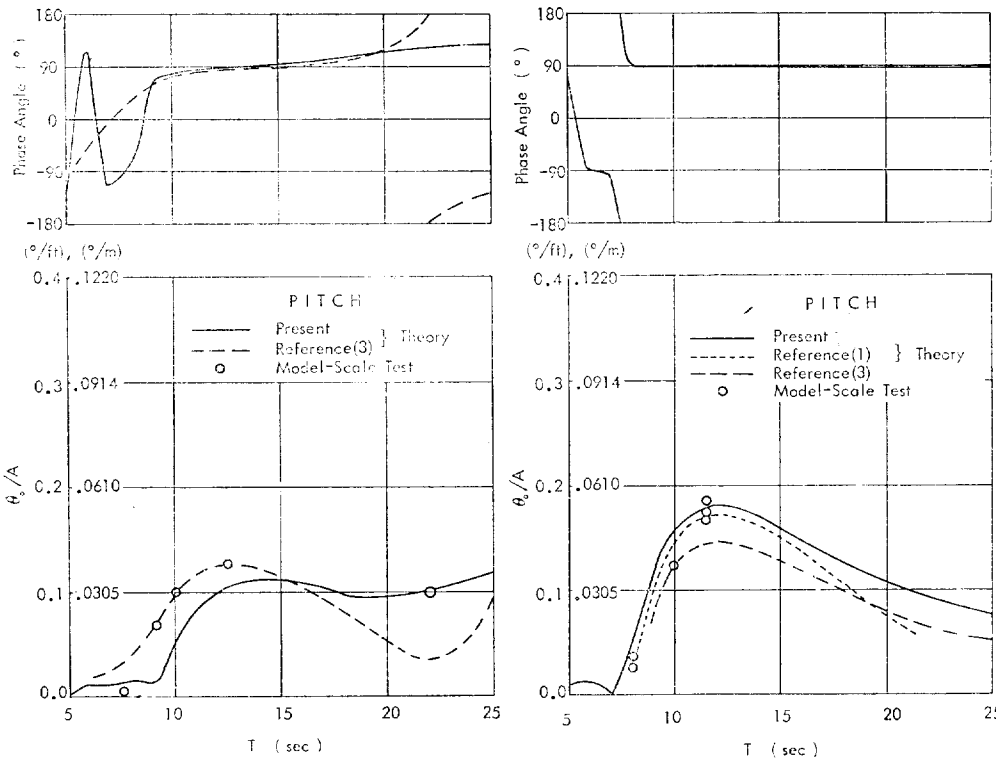

Fig. 10 Pitch of SEDCO 135-F (waves 30° off bow; deep water)
Fig. 11 Pitch of MOHOLE (head waves; deep water)

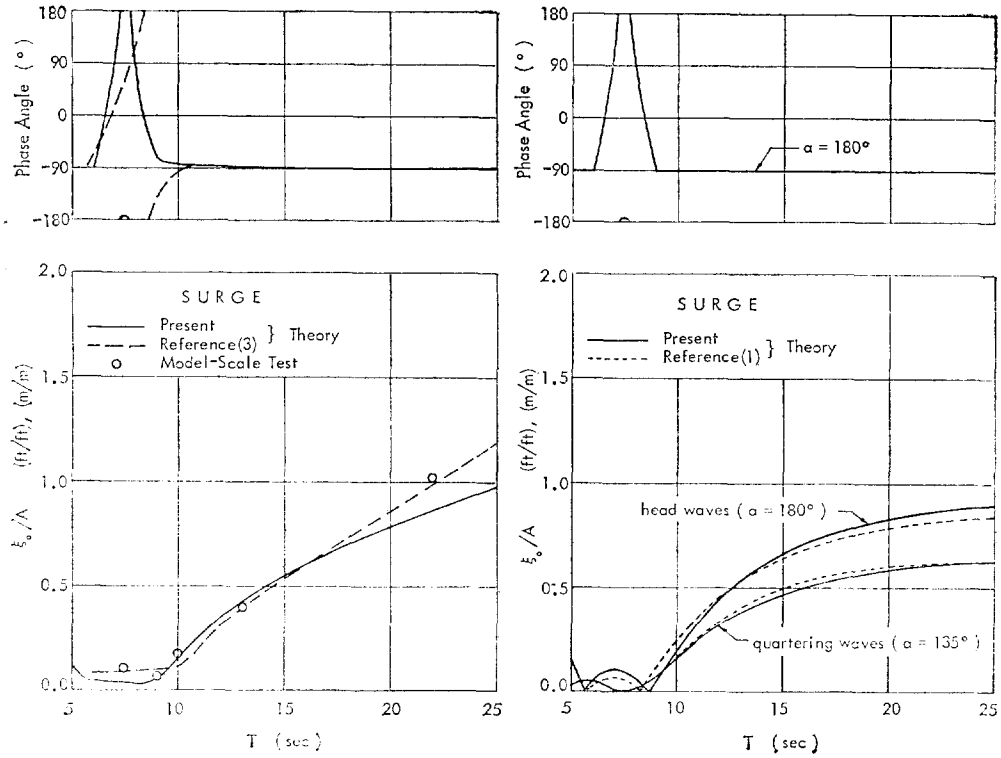

Fig. 12 Surge of SEDCO 135-F (waves 30° off bow; 400ft (121.92m) water depth)
Fig. 13 Surge of MOHOLE (head and quartering waves; deep water)

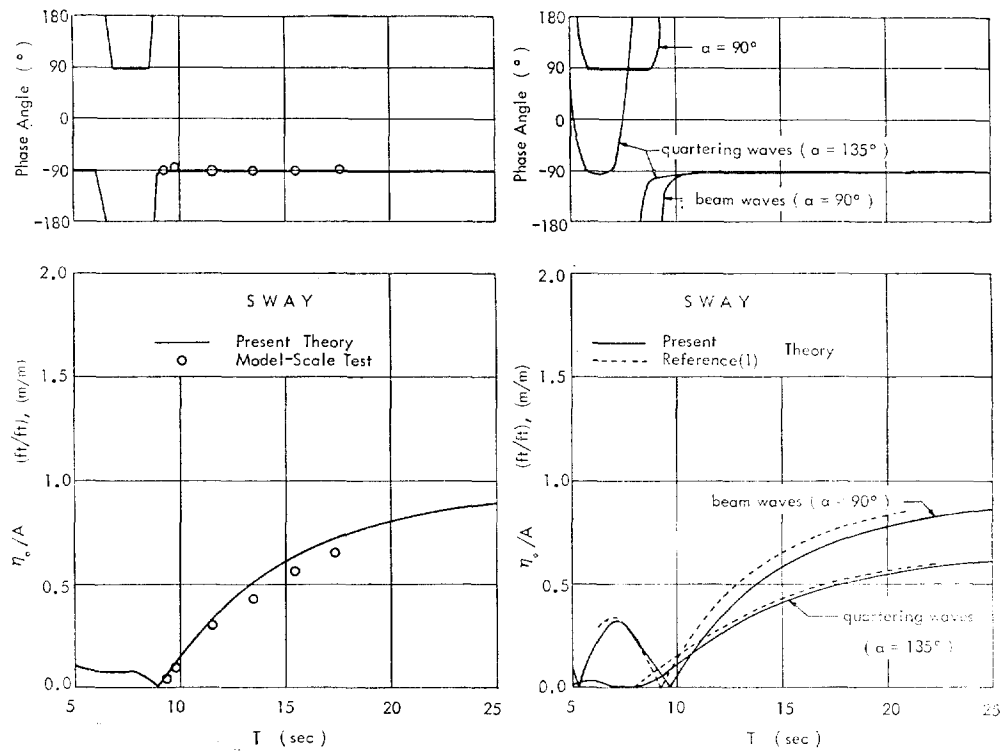

Fig. 14 Sway of SEDCO 135-F (beam waves; deep water)
Fig. 15 Sway of MOHOLE (beam and quartering waves; deep water)

steady state values, $(x_j)_o/A$ from the following expression,

$$\frac{X_j}{A}=\frac{(X_j)_o}{A}\cos(\omega t-\varepsilon_j), \qquad j=1,2,\cdots, 6 \qquad (57)$$

where ϵ_j are phase angles in degree as indicated in Figs. 6 to 16. The phase angles of motions are positive when the motions lag the wave, with the wave crest being at the rig CG as a reference.

Motion Comparison and Discussions. To test the present method's validity and accuracy in determining floating-rig motions in regular waves, motions predicted for the SEDCO 135-F rig in waves of 400 ft (121.92m) water depth were compared with motions measured by model-scale tests [3] and full-scale heave tests [9]. Also, motions predicted for the MOHOLE rig in waves of deep water with the model-scale test data [12]. Comparison shows good agreement of the present SEDCO 135-F heave predictions with both the model-scale test data and the full-scale test data over the wave period range of practical interest (Fig. 6). Fig. 7 through 16 for both rigs show good agreement between the present predictions and measured data for both amplitudes and phase a ngles of heave, roll, pitch, surge, sway, and yaw motions. Finally, comparisons of the present predicted motions (Figs. 7 to 16) with the Reference [3] and partly with the Reference [1] show that the present calaulations are more accurate for both motion amplitudes and phase angles. Usually wave components of T=5 to 15 sec are of interest for the drilling operations at sea, and waves of T>15 sec are of great interest for the survival conditions. Wave components of perhaps T>25 sec are very rare at sea. For the present two rigs, only the heave has its natural period below T=25 sec, and roll, pitch, surge, sway and

Table 1 Particulars of "MOHOLE" and "SEDCO 135-F" Rigs Used For the Motion Calculations

		MOHOLE	SEDCO 135-F (est.)
Displacement	(L. tons)	22,813.0	17,657.0
	(M. tons)	24,337.0	17,978.0
Draft	(ft)	70.0 (21.34)*	80.0 (24.38)
VCG	(ft)	67.5 (20.57)	
Radii of gyration			
r_x	(ft)	108.8 (33.16)	
r_y	(ft)	101.6 (30.97)	109.0 (33.22)
r_z	(ft)	119.9 (36.55)	
Column diameter	(ft)	31.0 (9.14)	35.0 (10.67)
Hull diameter	(ft)	35.0 (10.67)	
Effective hull length	(ft)	340.0 (103.63)	100.0 (30.48)
Hull height	(ft)	.....	25.0 (7.62)
Hull width	(ft)	.....	60.0 (18.29)
Column spacing	(ft)	130.0 (39.624)	280.0 (85.344)
Hull spacing	(ft)	215.0 (65.532)	280.0 (85.344)
Approx. steel weight**			
	(L. tons)	9,821.0	7,464.0
	(M. tons)	10,000.0	7,600.0

*Numbers inside the parentheses are in metric unit.
**Exclude variable deck load.

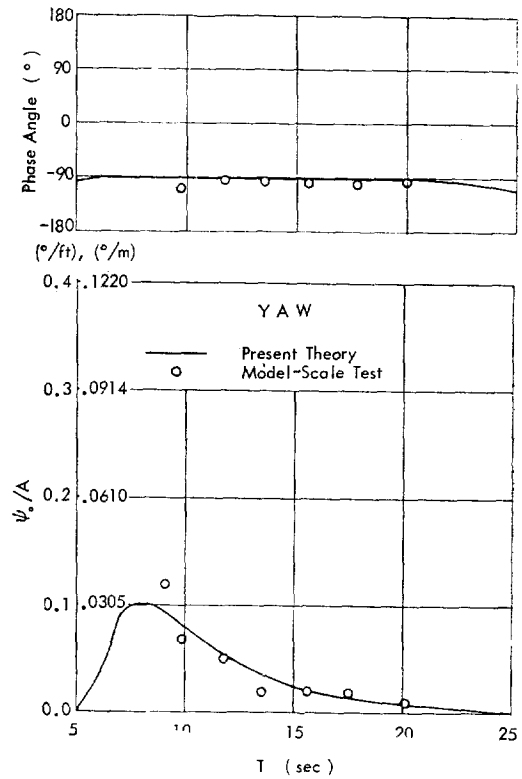

Fig. 16 Yaw of SEDCO 135-F (beam waves; deep water)

yaw have their natural periods beyond T=25 sec.

The total wave force components acting on the submerged portion of each bracing member are small as compared with the force components acting on each main hull and column member. Tests with the present analytical calculation with and without bracing members of both rigs showed little hydrodynamic influence of the bracing members on the calculated motions.

Heave. Figure 6 shows that the present heave prediction for the SEDCO 135-F rig for infinitely deep water agrees well over the wave period range with the model-scale test data obtained for the same condition and agrees reasonably well with the full-scale data measured for the various water depths. Note that the full-scale data [9] did not encounter the wave period range outside that indicated in Fig. 6. Figure 7 also shows that the present heave calculation for the MOHOLE rig is more accurate than the Reference [3]. The viscous damping coefficient for the present two rig members is empirically selected as $C_d=1.0$ (Figs. 6 and 7), since it gives good agreement between the present motion calculations and the model test results near the heave resonance. The larger the damping forces, the smaller the heave amplitude near its resonance period. Submerged member's surface of the full-scale rig is usually rougher due to marine fouling than that of the scaled model, and consequently viscous damping force is expected to be larger for the full-scale rig; that is, the heave resonance amplitude is expected to be smaller than for the scaled model. The heave and sway added mass coefficients used for the present SEDCO 135-F calculation at the drilling draft (or s/a=6.4) are 0.85 and 0.4 respectively, and the corresponding wave damping coefficients are zero (Fig. 4). The heave and sway added mass coefficients used for the MOHOLE calculations at its drilling draft (or s/a=3.0) are given in Fig. 5. The added mass coefficients given in Figs. 4 and 5 are frequency-dependent due to the free surface effect and larger for finite-depth water than for deep water [4]-details are discussed above.

Though not presented in this paper, comprehensive analysis [4] of the present method shows that a change of the wave direction relative to the rig heading does not significantly alter the heave amplitudes of most semisubmersible rigs, but can significantly influence the heave phase angles. The wave period at which the minimum heave amplitude occurs at T< 10 sec depends on the column spacing and the distance between the hulls in beam waves, and on the column spacing and the hull lengths or sizes in head waves. For the present calculations, wave amplitudes used are A=15ft (4.572m). Variations of the wave amplitudes for the present calculations change the heave amplitudes near resonance through the viscous damping term in Eq. (6).

Other Modes of Motion. The present roll (Figs. 8 and 9) and pitch (Figs. 10and 11) predictions for both rigs give good agreement with the model-scale test data and clearly show better accuracy of roll predictions, as compared with the References [1, 3, 12]. Although not presented here, comprehensive motion analyses [15] show non-zero pitch for beam waves. This is because the SEDCO 135-F rig has three columns and hulls (or pontoons) which are not symmetric about the y-axis when the incident waves act on the submerged members of the rig. On the other hand, many existing floating semisubmersible drilling rigs such as the MOHOLE have near symmetry about both the x-and y-axes, and amplitudes of the roll for the head waves and pitch for the beam waves are zero.

Surge (Fig. 12) and sway (Fig. 14) predictions for the SEDCO 135-F rig agree well with the model-scale test data. Model test data of surge and sway for the MOHOLE rig do not exist. Unlike ships' surge and sway, the surge in head waves and sway in beam waves are nearly the same on the order of magnitude of the amplitude for the present rigs and most column-stabilized semisubmersible rigs at their drilling drafts.

Comparison of yaw motions in the present calculation and the model-scale test data gives good agreement in both the amplitude and phase angle (Fig. 16). This good agreement of yaw partly supports the assumption made above that the hydrodynamic end effect of the rig members can be neglected in the motion calculation. Fig. 16 also shows that the present prediction accuracy of yaw is better than the Reference [3]. There exist no yaw test data for the MOHOLE rig.

For the modes of motion other than heave, the effects of the added mass and damping on motions

are very small over the frequency range of interest. This is because the added mass and damping forces significantly influence the motions only near the resonance periods and except for heave, the motion resonance occur at T>25 sec which has little practical significance. Ocean waves rarely possess wave components of T=25 sec. Therefore, for the modes of many floating structures' motion other than the heave, motion resonance periods are longer than perhaps 25 seconds, and small errors in the added mass and damping coefficients in the equations of motion affect little of the accuracy of the calculated motions.

Motions for Irregular Waves

The motions obtained for regular waves are used to predict response energy spectra and statistical values for motions in a given sea, using spectral analysis. The response motions obtained as transfer functions $R_r(\omega)$ in regular waves must be the same for the same rig in different irregular sea states under the previous assumption that wave slope is small and responses are linear. We can apply the proper wave stectrum for a specific seaway in a specified season to $R_r(\omega)$ to get motion energy spectra for irregular sea. This statistical analysis does not give time history of the responses, but gives statistical description of the motions which can be used in preliminary design of a rig.

It is assumed, that the irregular seaway and the response motions are random processes, that the random processes are represented by a stationary Gaussian distribution, and that the sum of the motions in response to a number of simple regular waves is equal to the motion responses to the sum of waves-linear superposition principle [7]. Under these assumptions, the rigs' motion response energy spectrum $R_s(\omega)$ can be represented by

$$R_s(\omega)=S_1(\omega)R_r^2(\omega) \tag{58}$$

where $S_1(\omega)$ is a unidirectional ocean wave spectrum energy density and $R_r(\omega)$ is a motion transfer function such as given in Figs. 6 to 16.

Integration of $S_1(\omega)$ over the frequency gives wave energy E_1, and the integration of $R_s(\omega)$ over the frequency gives motion energy E_r for the seaway $S_1(\omega)$. Based on the results of Longuet-Higgins [5], significant wave height (an averaged value of the 1/3-highest wave heights) and significant motion in double amplitude respectively can be obtained,

$$H_{1/3}=4.0\sqrt{E_1} \tag{59}$$

and

$$R_{1/3}=4.0\sqrt{E_r} \tag{60}$$

One of the statistical ocean wave representations is the Pierson-Moskowitz wave energy spectrum [6] which is defined as

$$S_1(\omega)=\frac{C}{\omega^5}e^{-k/w^4} \tag{61}$$

where

$C=0.0081g^2$

g=gravity acceleration in ft/sec^2

ω=wave frequency in rad/sec

$k=32.38/H_{1/3}^2$

$H_{1/3}$=the 1/3 highest averaged (significant) wave height in ft.

This spectrum is the result of the analysis of wave data measured for a long period of time in the North Atlantic Ocean.

Using the Pierson-Moskowitz wave spectrum for the $S_1(\omega)$-see Table 2 and Fig. 18, significant heaves ($\zeta_{1/3}$) in double amplitude (Fig. 18) are calculated with the heave energy spectrum $R_s(\omega)$ for the $R_r(\omega)$ of heave of Fig. 7. Figure 17 shows calculated significant heave in double amplitude for the irregular waves represented by the Pierson-Moskowitz wave spectra. In Fig. 18, the wave energy densities $S_1(\omega)$

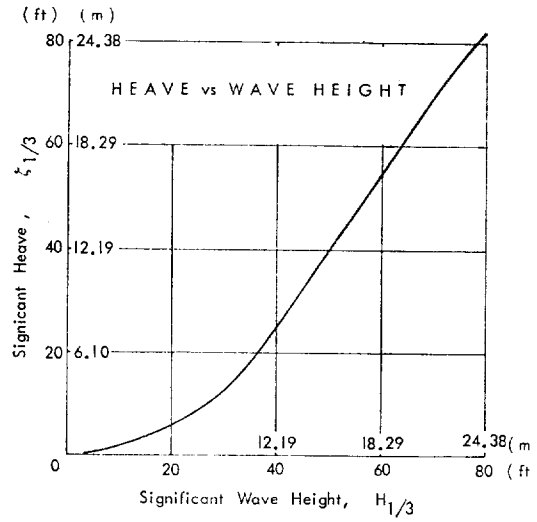

Fig. 17 Significant Heave Versus Significant Wave Heights for the MOHOLE Rig (beam waves; deep water)

are obtained for the given significant wave heights as indicated, and the shaded portion is the heave motion energy spectra $R_r(\omega)$ calculated with Eqs. (58) and (61) for the MOHOLE heave transfer function $R_r(\omega)$ given in Fig. 7; the significant wave height used is $H_{1/3}$=30ft (9.144m). The significant heaves ($\zeta_{1/3}$) in Fig. 17 are calculated with Eq. (60) for the various $H_{1/3}$ indicated in the Figure.

Usually this statistical analysis of motions for the irregular waves has been a simple and practical

TABLE 2 Pierson-Moskowitz Wave Spectrum

Sea tate	Significant Wave Height (ft)	Signficant Range of Periods (sec)	Period of Maximum Energy (sec)	Average Wave Period (sec)	Average Wavelength (ft)
0	0.10	0.34— 1.09	0.87	0.62	1.31
0	0.15	0.42— 1.33	1.07	0.76	1.97
1	0.50	0.77— 2.43	1.95	1.39	6.57
1	1.00	1.09— 3.43	2.76	1.96	13.14
1	1.20	1.19— 3.76	3.02	2.15	15.76
2	1.50	1.34— 4.21	3.38	2.40	19.70
2	2.00	1.54— 4.86	3.90	2.77	26.27
2	2.50	1.72— 5.43	4.36	3.10	32.84
2	3.00	1.89— 5.95	4.78	3.40	39.41
3	3.50	2.04— 6.43	5.16	3.67	45.98
3	4.00	2.18— 6.87	5.52	3.92	52.54
3	4.50	2.31— 7.29	5.86	4.16	59.11
3	5.00	2.44— 7.68	6.17	4.38	65.68
4	6.00	2.67— 8.41	6.76	4.80	78.82
4	7.00	2.89— 9.09	7.30	5.19	91.95
4	7.50	2.99— 9.41	7.56	5.37	98.52
5	8.00	3.08— 9.71	7.81	5.55	105.09
5	9.00	3.27—10.30	8.28	5.88	118.22
5	10.00	3.45—10.86	8.73	6.20	131.36
5	12.00	3.78—11.90	9.56	6.79	157.63
6	14.00	4.08—12.85	10.33	7.34	183.90
6	16.00	4.36—13.74	11.04	7.84	210.17
6	18.00	4.63—14.57	11.71	8.32	236.45
6	20.00	4.88—15.36	12.34	8.77	262.72
7	25.00	5.45—17.17	13.80	9.80	328.40
7	30.00	5.97—18.81	15.12	10.74	394.08
7	35.00	6.45—20.32	16.33	11.60	459.76
7	40.00	6.90—21.72	17.46	12.40	525.43
8	45.00	7.32—23.04	18.52	13.15	591.11
8	50.00	7.71—24.28	19.52	13.87	656.79
8	55.00	8.09—25.47	20.47	14.54	722.47
8	60.00	8.45—26.60	21.38	15.19	788.15
9	70.00	9.12—28.73	23.09	16.41	919.91
9	80.00	9.75—30.72	24.69	17.54	1050.87
9	90.00	10.35—32.58	26.19	18.60	1182.23
9	100.00	10.91—34.34	27.60	19.61	1313.59

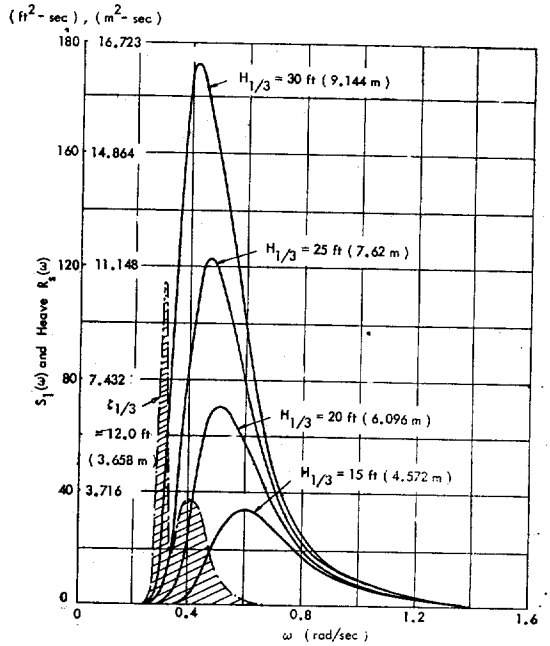

Fig. 18 The Pierson-Moskowitz Wave Spectrum and a Heave Motion Spectrum of the MOHOLE Rig

method in design. Nonlinearity problem exists for high sea states, can not be presently solved for practical use, and is not discussed here, since it is beyond the scope of the present paper.

REFERENCES

1. Bain, J.A., "Extension of Mohole Platform Force and Motion Studies," Project Mohole Report by General Electric Co. (October, 1964).
2. Blagoveshchensky, S.N., *Theory of Ship Motions*, Dover (1962).
3. Burke, B.G., "The Analysis of Motions of Semi-submersible Drilling Vessels in Waves," *Proceedings*, Offshore Technology Conference, Houston, Texas (April, 1969), Paper No. 1024.
4. Chung, J.S., "Unpublished paper." (1974).
5. Longuet-Higgins, M.S., "On the Statistical Distribution of the Heights of Sea Waves," *Journal*, Marine Research, Vol. 2, No. 3 (1952), pp. 245—265.
6. Pierson, W.J., and Moskowitz, L., "A Proposed Spectral Form for Fully Developed Wind Seas Based on the Similarity Theory of S.A. Kitaigorodskii," *Journal*, Geophysical Research, Vol. 69, No. 24 (Dec. 15, 1964).
7. St. Denis, M. and Pierson, W.J., "On the Motion of Ships in Confused Seas, "*Transactions*, The Society of Naval Archicects and Marine Engineers, Vol. 61 (1953).
8. Kim, C.H. and Chou, F., "Motions of a Semi-Submersible Drilling Platform in Head Seas," Davidson Laboratory Report, OE 71-8 (Dec. 1971).
9. Watts, J.S., et al., "A Performance Review of the SEDCO 135-F Semisubmersible Drilling Vessel," *Proceedings*, Petroleum Society of CIM. Calgary, Canada (May, 1968).
10. Hooft, J.P., "A Mathematical Method of Determining Hydrodynamically Induced Forces on a Semi-Submersible," *Transaction*, SNAME (1971).
11. Frank, W., "Oscillation of Cylinder In or Below the Free Surface of Deep Fluids," Naval Ship R & D Center Report 2357 (1967).
12. McClure, A. C., "Development of the Project MOHOLE Drilling Platform," *Transaction*, SNAME (1965), p. 50-99.
13. Paulling, J.R. and Horton, E.E., "Analysis of the Tension Leg Platform." *Proceedings*, Offshore Technology Conference, Houston, Texas (1970), OTC paper 1263.
14. Morison, J.R., et al., "Experimental Studies of Forces on Piles," *Proceedings*, First Conference on Coastal Engineering, ASCE, pp. 340—369.
15. Chung, J.S., "Motions of Floating Structures in Finite-Depth Water," to be published (1975).
16. Hwang, J.H., et al., "On the Heave Oscillation of a Circular Dock," *Journal*, SNA Japan, Vol. 130 (1971), pp. 121-130.